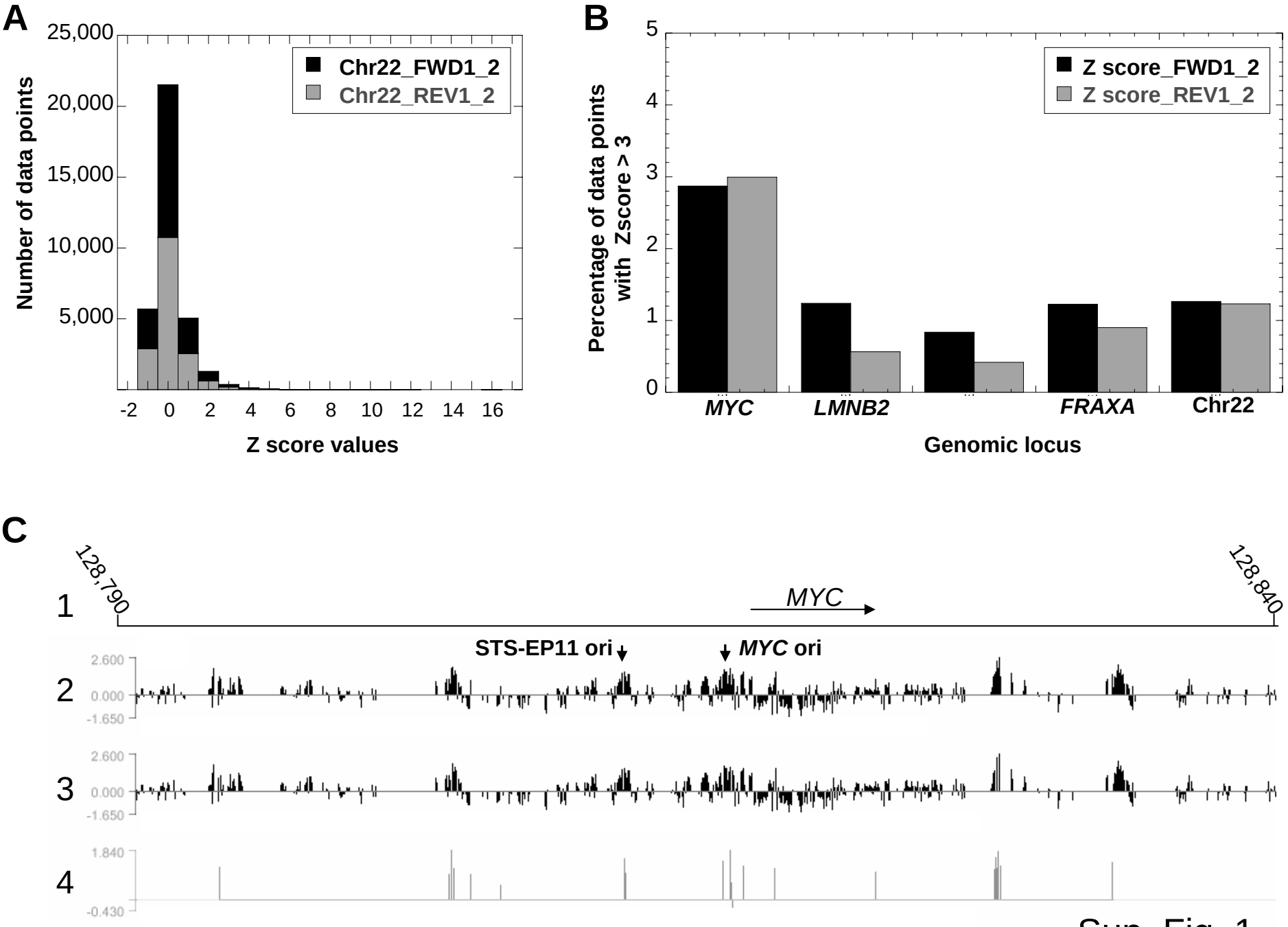
A
25,000
20,000
15,000
10,000
5,000
Number of data points
Chr22_FWD1_2
Chr22_REV1_2
-2
0
2
4
6
8
10
12
14
16
Z score values
B
5
4
3
2
1
0
Percentage of data points with Zscore > 3
Z score_FWD1_2
Z score_REV1_2
MYC
LMNB2
FRAXA
Chr22
Genomic locus
C
128,790
128,840
1
MYC
STS-EP11 ori
MYC ori
2
2.600
0.000
-1.650
3
2.600
0.000
-1.650
4
1.840
-0.430

Sup. Fig. 1

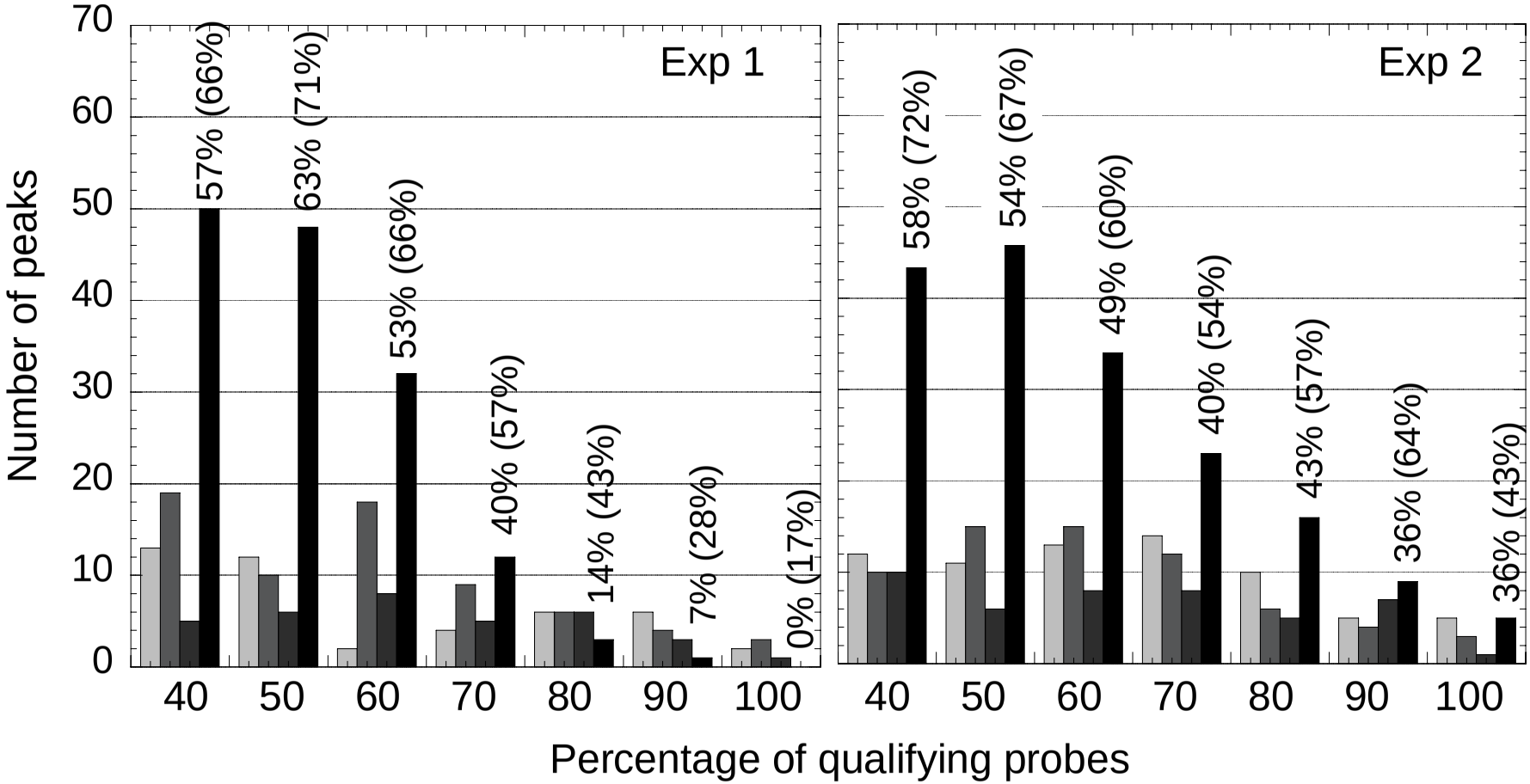
Exp 1
Exp 2
Number of peaks
Percentage of qualifying probes
0
10
20
30
40
50
60
70
40
50
60
70
80
90
100
57% (66%)
63% (71%)
53% (66%)
40% (57%)
14% (43%)
7% (28%)
0% (17%)
58% (72%)
54% (67%)
49% (60%)
40% (54%)
43% (57%)
36% (64%)
36% (43%)

Sup. Fig.2

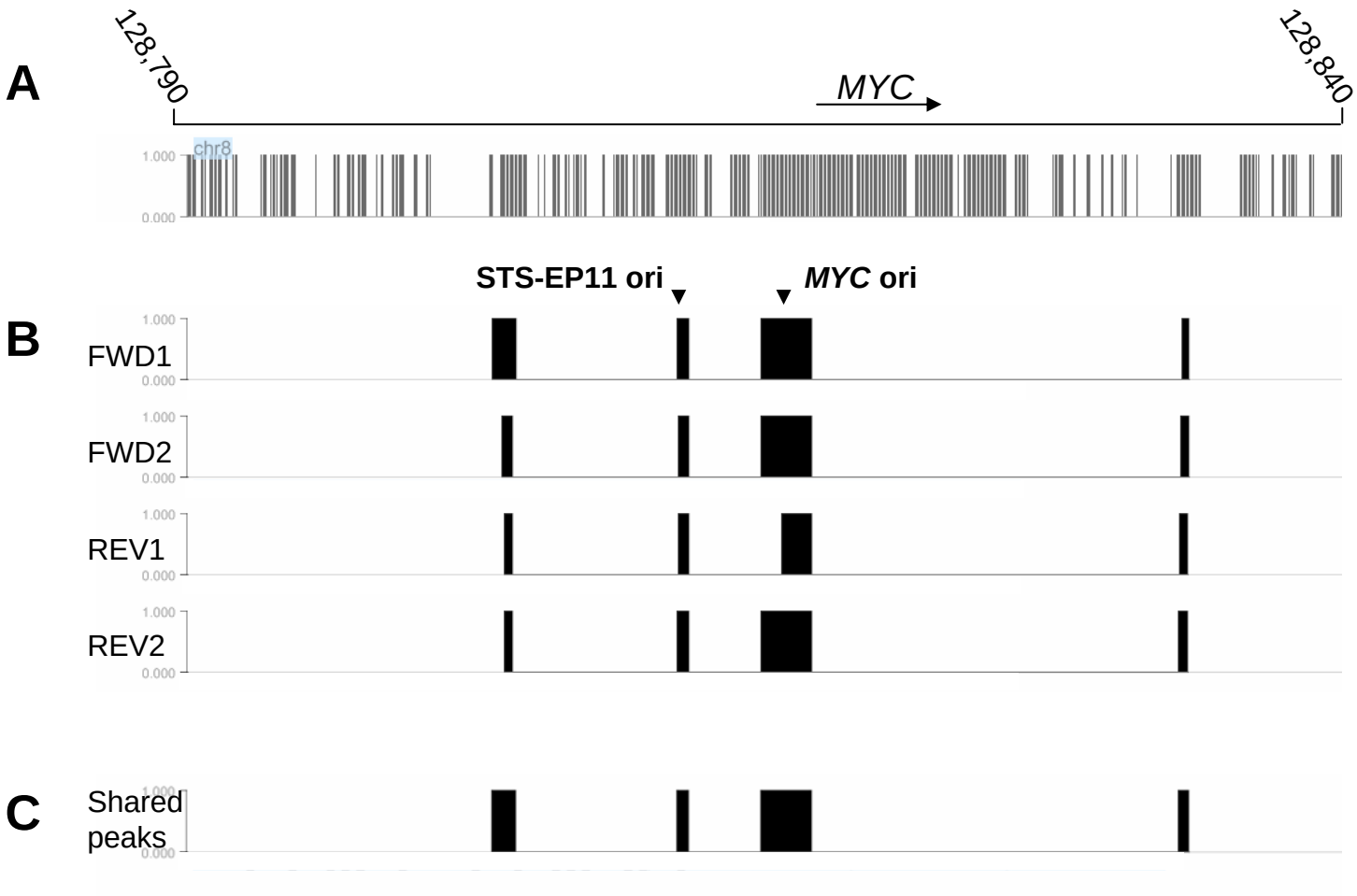
A
128,790
MYC
128,840
chr8
1.000
0.000
STS-EP11 ori
MYC ori
B
FWD1
FWD2
REV1
REV2
C
Shared peaks

Sup. Fig.3

Chr22 region

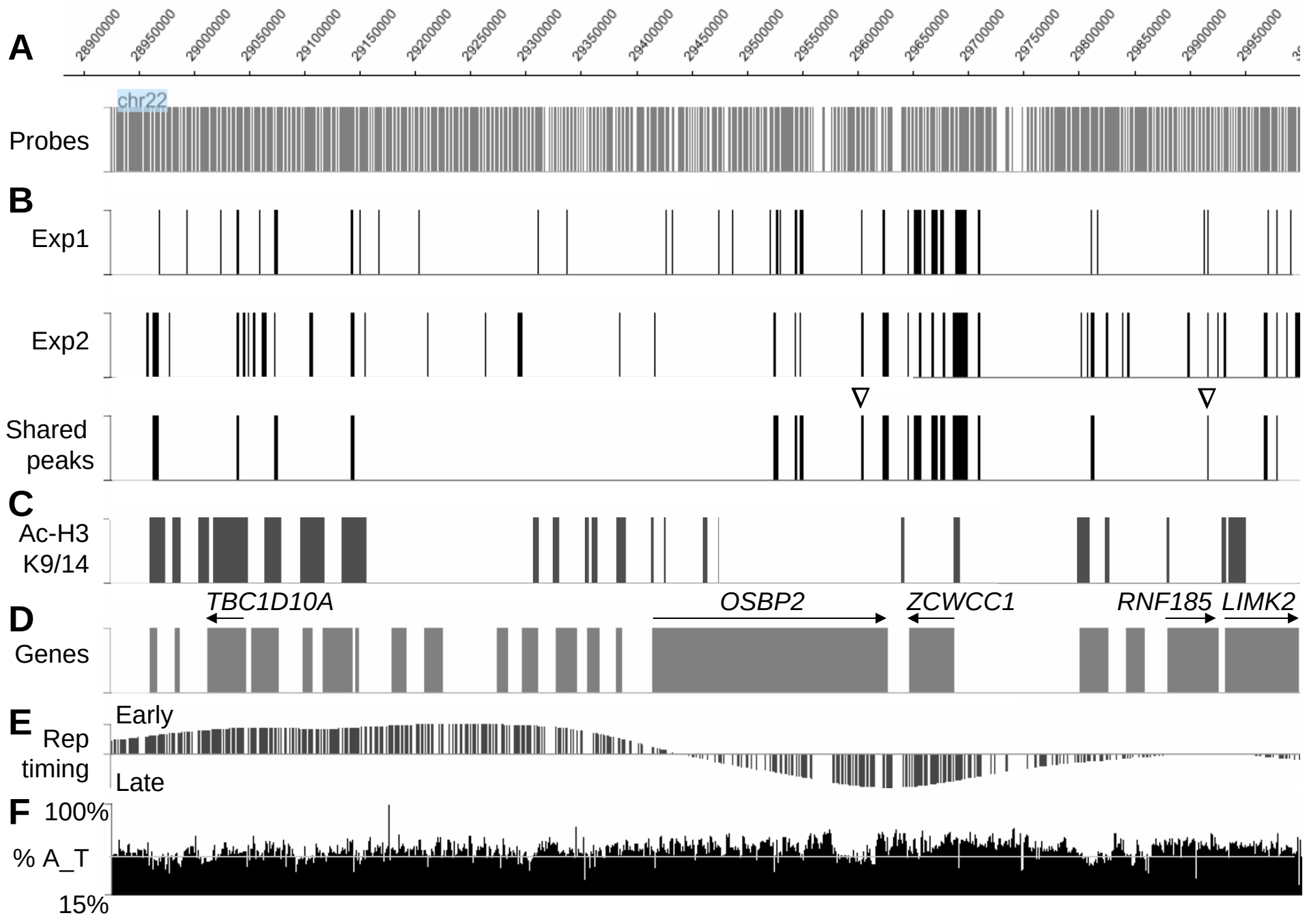

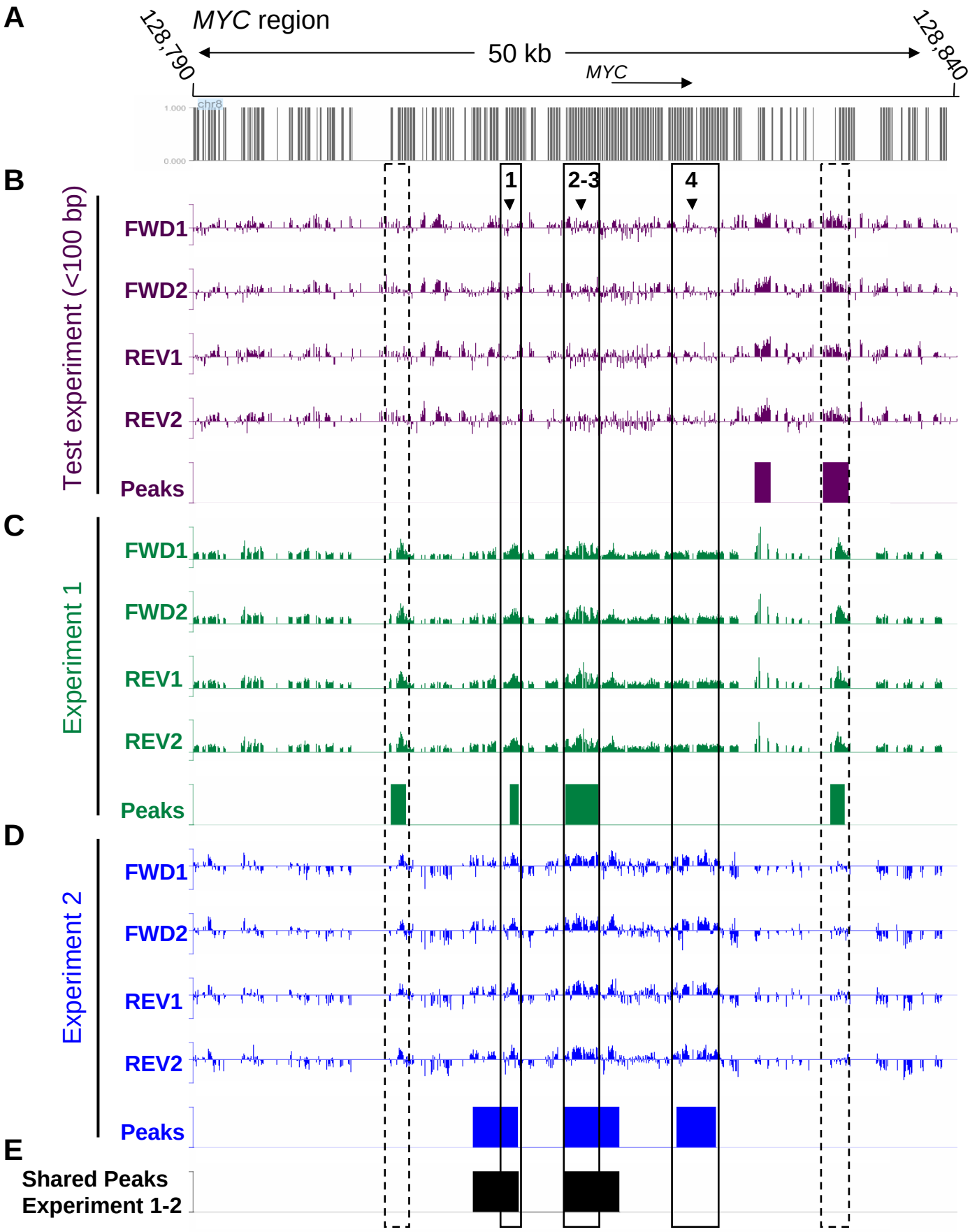
A
MYC region
128,790
50 kb
128,840
MYC
chr8
1.000
0.000
B
Test experiment (<100 bp)
1
2-3
4
FWD1
FWD2
REV1
REV2
Peaks
C
Experiment 1
FWD1
FWD2
REV1
REV2
Peaks
D
Experiment 2
FWD1
FWD2
REV1
REV2
Peaks
E
Shared Peaks
Experiment 1-2

Sup. Fig. 5

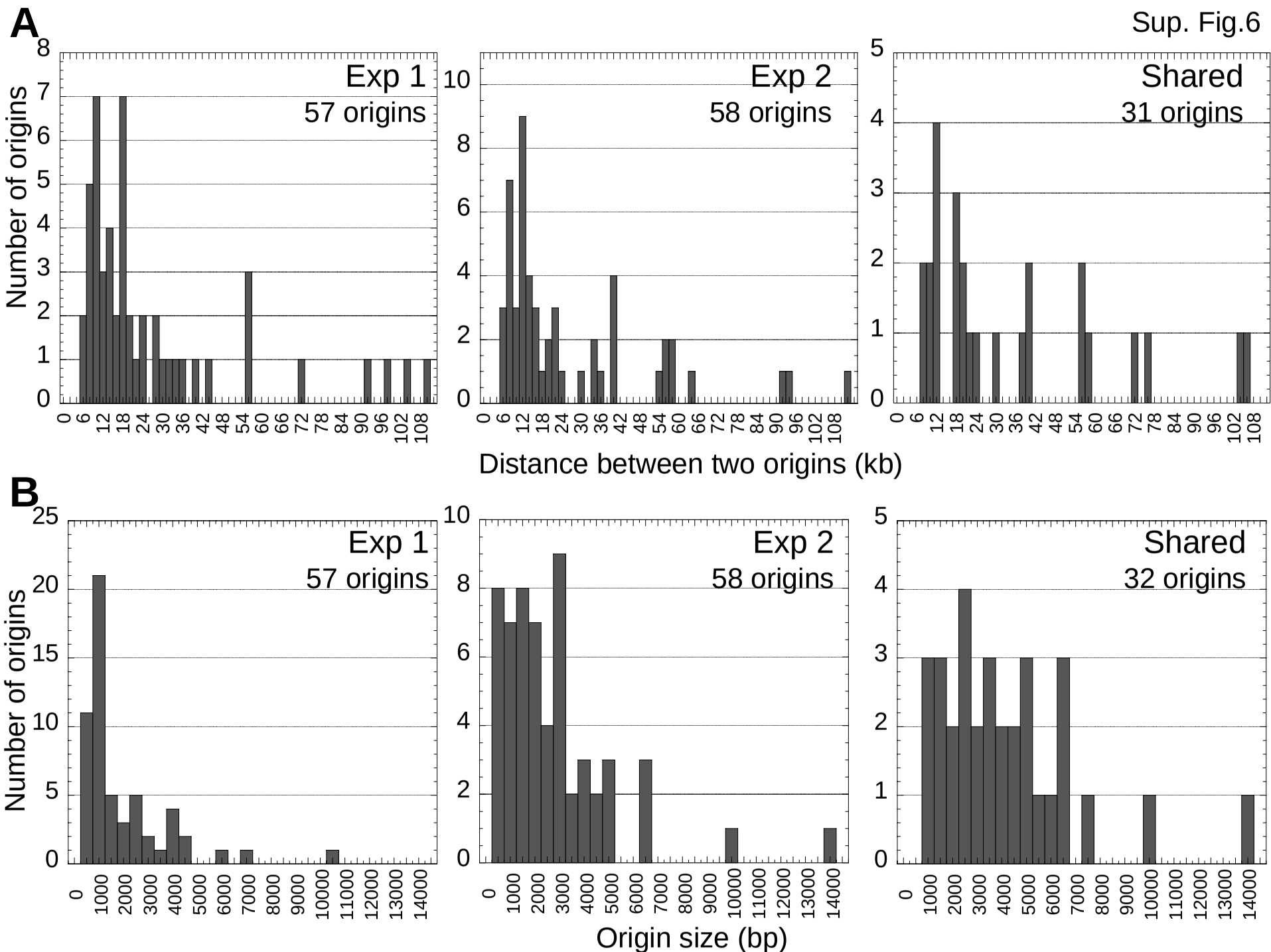
A
Exp 1
57 origins
Exp 2
58 origins
Shared
31 origins
Number of origins
Distance between two origins (kb)
B
Exp 1
57 origins
Exp 2
58 origins
Shared
32 origins
Number of origins
Origin size (bp)

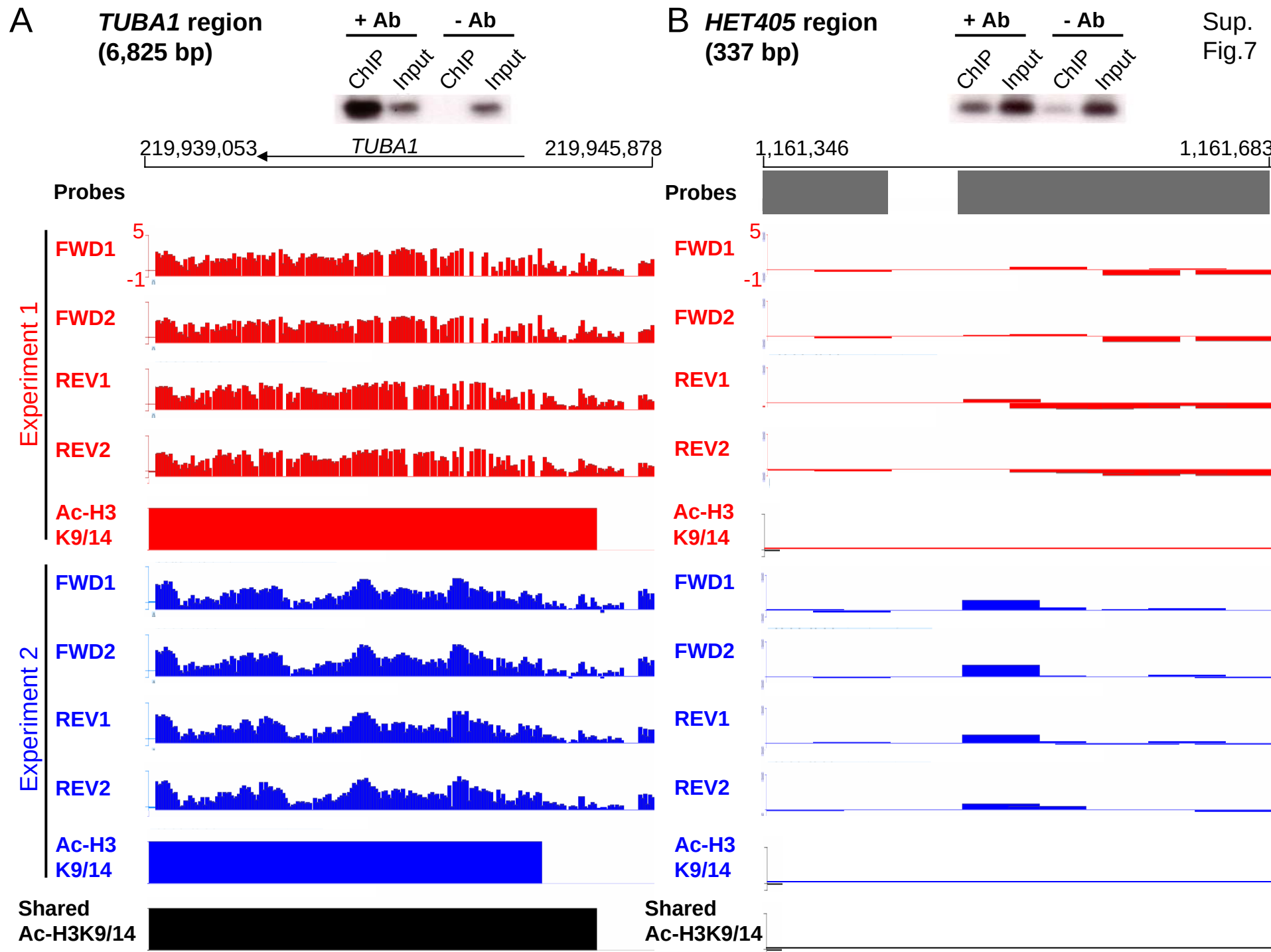
A
TUBA1 region
(6,825 bp)
+ Ab
- Ab
ChIP
Input
ChIP
Input
219,939,053
TUBA1
219,945,878
Probes
Experiment 1
FWD1
FWD2
REV1
REV2
Ac-H3
K9/14
5
-1
Experiment 2
FWD1
FWD2
REV1
REV2
Ac-H3
K9/14
Shared
Ac-H3K9/14
B
HET405 region
(337 bp)
+ Ab
- Ab
ChIP
Input
ChIP
Input
1,161,346
1,161,683
Probes
FWD1
FWD2
REV1
REV2
Ac-H3
K9/14
5
-1
FWD1
FWD2
REV1
REV2
Ac-H3
K9/14
Shared
Ac-H3K9/14
Sup.
Fig.7

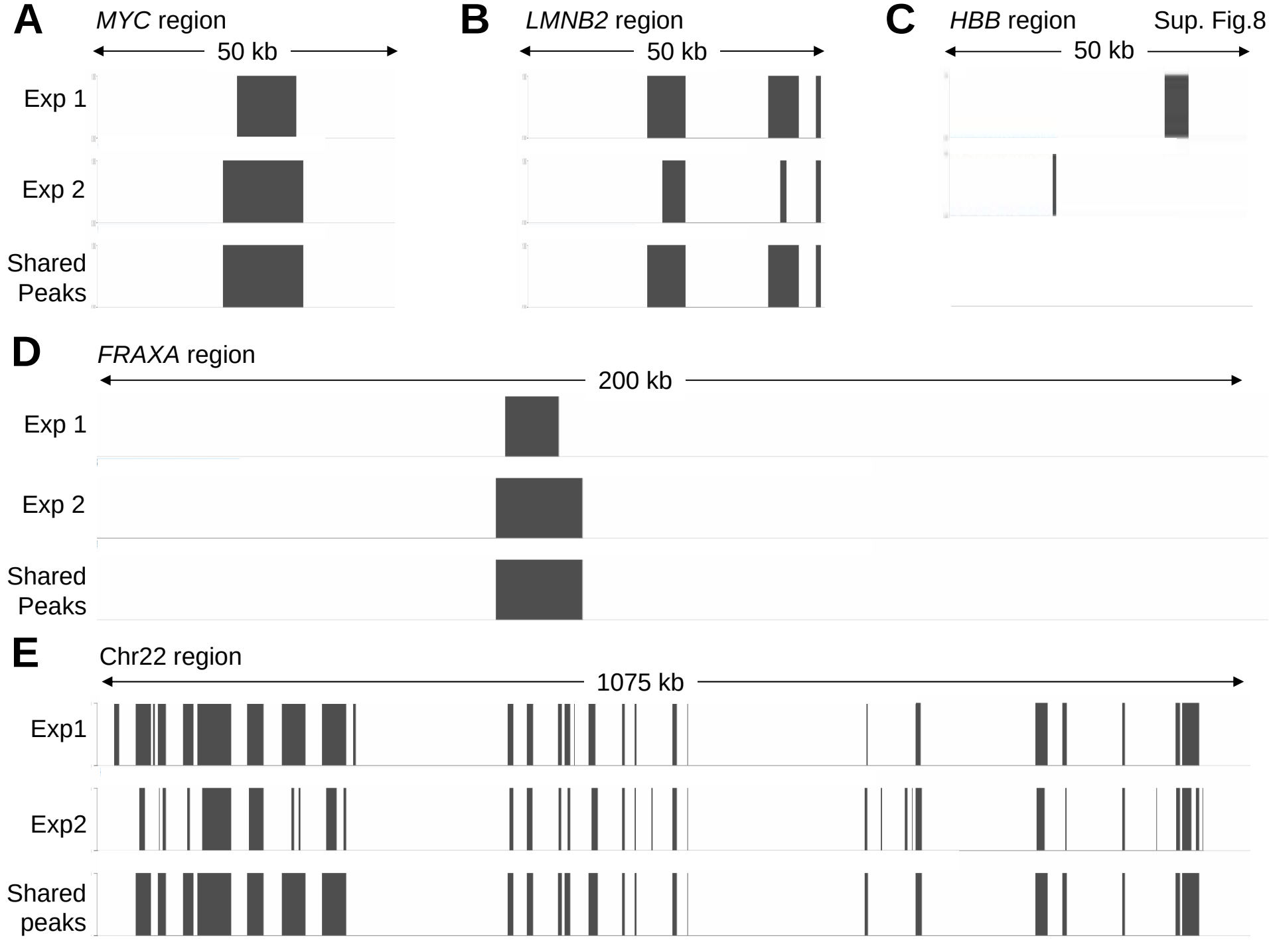
A
MYC region
50 kb
Exp 1
Exp 2
Shared Peaks
B
LMNB2 region
50 kb
C
HBB region
Sup. Fig.8
50 kb
D
FRAXA region
200 kb
Exp 1
Exp 2
Shared Peaks
E
Chr22 region
1075 kb
Exp1
Exp2
Shared peaks

Supplementary Figure Legends

Supplementary Figure 1. Zscore analysis of the microarray data. (A) Distribution of the Z score values obtained for the forward (FWD, in black) and reverse (REV, in grey) duplicated probe sets for the chr22 region. Less than 1% of the FWD and REV probes had a Z score ≥4. (B) The percentage of data points excluded from the analysis for the FWD (black) and REV (grey) duplicated probe sets when using a cut-off of 3 for the Z score. Of note, ~88% of the Z score values were below 1 (C) (1) Chromosome coordinates along the 50 kb *MYC* region represented on the array. (2) Example of the microarray results for the *MYC* region before the Z score analysis, and (3) after removing all data points with a Z score >3. (4) Location of the data points removed. In panel 2, the arrowheads mark the location of two known origins in the *MYC* region. The different programs developed in this study for Z score transformation as well as for the subsequent analyses are available upon request.

Supplemental Figure 2. Distribution of all of the peaks for experiments 1 and 2 with an FPR≤10% present in one (light gray), two (medium gray), three (dark grey), or four (black) of the data sets, for each percentage of qualifying probes (40%-100%) within the 625 nt sliding window used in the analysis. The percentage of peaks found in four of the data sets is indicated above each black bar. The cumulative percentage of peaks present in both three and four of the data sets, which we considered as potential origins, is given in parenthesis. Of note, more than 90% of the putative origins were found when 40% was used as the cut-off for the number of qualifying probes. The remaining 10% were only observed with an FPR≤10% at a higher cut-off. As expected, the total number of peaks, as well as the number of peaks found in at least three data sets, decreased with the increasing cut-off value. To examine the impact of the density of probes on the feasibility of mapping origins, we decreased the number of probes on our array

in silico from a density of 30 nt from the start of one probe to the start of the next probe, to 120 nt by increments of 30 nt, and applied the peak finding method. This analysis revealed that the number of known origins that were not detected increased with decreasing density of probes (data not shown).

Supplementary Figure 3. Location of the putative origins for the four data sets for the *MYC* region. (A) The upper panel shows the chromosome coordinates, as well as the location of the probes present on the microarray. (B) Each track (FWD1, FWD2, REV1, and REV2) displays the location of the origin peaks found in experiment 1, using a cut-off of 40% of qualifying probes within the sliding window, for each of the data sets after applying the "2 kb-rule" merging method. (C) The track indicates the location of the origin peaks that are shared by the four data sets.

Supplemental Figure 4. Location of origins, chromatin acetylation peaks and genes, replication timing and AT content maps for the chr22 region. (A) Chromosome coordinates and location of the probes present on the microarray. (B) location of origins identified in the two independent experiments 1 and 2, and shaed origins. (C) location of the acetylated chromatin loci (histone H3 K9/14) shared between two independent ChIP experiments. (D) Location of the annotated genes. (E) Timing of replication analysis (Early vs. Late replication) using microarray analysis (White et al., 2004). (F) Percentage of chromosomal AT content. In panel E, the $\log_2$ ratio of (early/late newly-replicated DNA hybridization signals) is plotted on the y axis. In panel F, the AT content is plotted as a 500 bp-sliding window along the region, and 50% AT content is indicated by a horizontal white bar. The open arrowheads in (B) indicate the putative origins tested by real-time PCR analysis.

Supplemental Figure 5. Specificity of the high-throughput origin mapping method. (A) The upper panel indicates the chromosome coordinates, and the location of the probes for the *MYC* region. The microarray results (FWD1, FWD2, REV1, and REV2, Z score≤3) as well as the origin peaks detected are shown for the following three experiments: (B) a test experiment (purple) using nascent strand highly-enriched for Okazaki fragments (smallest fragments <100 bp), (C and D) two independent nascent strand isolations using larger nascent strand DNAs (300-1000 bp). Of note, the nascent strand population used in experiment 2 (blue) was slightly larger in size than the one used in experiment 1 (green). (E) The last track (black) indicates the positions of the origins shared between the two independent experiments 1 and 2. The left-most dashed line rectangle indicates the location of an origin found in experiment 1 only; based on the microarray results, this origin may be a false-negative origin in experiment 2. The right-most dashed line rectangle indicates the position of a peak detected in the test experiment and the experiment 1, but not in experiment 2. This result suggests that this origin is likely a false-positive origin in the experiment 1.

Supplemental Figure 6. (A) Distribution of the average distance between adjacent origins (center-to-center) for all five regions combined, for the two independent experiments 1 and 2 and the shared origins. The very large inter-origin distance (377 kb) on chr22 was not plotted on the graph for the shared peaks. In summary, 86% and 84% of the shared origins of experiment 1 and 2 respectively were ≤50 kb apart. (B) Distribution of the size of the origins from all five regions combined, for the two independent experiments 1 and 2, and the shared origins. The total number of origins analyzed is indicated in each graph.

Supplemental Figure 7. Specificity of the high-throughput chromatin acetylation mapping method. (A) The hyperacetylated region, *TUBA1*, and (B) the hypoacetylated region, *HET405*

were used as positive and negative controls, respectively, for our ChIP-on chip experiments. The specificity of the ChIP of Ac-H3 K9/14 verified by PCR, the chromosome coordinates, the location of the arrayed probes, the results (FWD1, FWD2, REV1, and REV2, Z score≤3) of the microarray data, the shared Ac-H3 K9/14 peaks for each independent ChIP experiment (1 and 2), and the shared Ac-H3 K9/14 peaks between the two independent ChIP experiments 1 and 2 are shown for each region. The control PCR was illustrated at the top performed on an equal volume of ChIP DNA and input DNA to amplify *HET405* (Forward primer: 5'-CAGAACTGTTTGTGATGTG-3', reverse primer: 5'-TGTAGTATCTGCAAGAGGAC-3', 35 cycles at 60 °C) and *TUBA1* (Forward primer: 5'-CAGATGCCCAGTGACAAGAC-3', reverse primer: 5'-AGTGTGAGAGAAACCCAGAC-3', 35 cycles at 60 °C). PCR products were resolved on a 1% agarose gel and transferred to the Hybond^{TM}-N+ membrane. Southern blot probes were produced by PCR amplification of the *TUBA1* and *HET405* sequences from genomic DNA, and subsequent gel purification and radioactive labeling. Band intensity was quantified by phosphor-imaging. The acetylation ratio was calculated as ChIP Intensity/(Input Intensity*100) since the input DNA was extracted from 1% of the starting lysate.

Supplemental Figure 8. Location of the Ac-H3 K9/14 peaks within the (A) *MYC*, (B) *LMNB2*, (C) *HBB*, (D) *FRAXA*, and (E) Chr22 regions for the independent ChIP experiments 1 and 2, as well as the Ac-H3 K9/14 peaks that are shared by both experiments.

Supplementary Table 1. Chromosomal Regions Covered on the Microarray Platform

Region	Chromosome	Start (bp)	Stop (bp)	Size (bp)
MYC	8	128,790,835	128,840,835	50,000
LMNB2	19	2,354,000	2,404,000	50,000
HBB	11	5,183,000	5,233,000	50,000
FRAXA	X	146,630,000	146,830,000	200,000
Chr 22	22	28,925,000	30,000,000	1,075,000
TUBA1	2	219,939,053	219,945,878	6,825
HET405	9	1,161,346	1,161,683	337

Supplementary Table 2. Origin Identified by Microarray Analysis

Region	Origins		Origin start (bp)	Origin end (bp)
MYC	Found in Experiment 1		128,803,756	128,804,765
			128,811,558	128,812,118
			128,815,174	128,817,331
			128,832,515	128,833,477
	Found in Experiment 2		128,809,111	128,812,058
			128,815,102	128,818,705
			128,822,431	128,825,027
	Shared by Experiment 1 and 2		128,809,111	128,812,118
			128,815,102	128,818,705
	Previously mapped origins	STS-EP11 ori (700-850 bp)	128,810,453	128,810,768
		MYC ori	128,815,936	128,816,304
		STS-I ori (615-850 bp)	128,818,950	128,819,106
		STS-J-M ori (615-1500 bp)	128,821,862	128,822,989
LMNB2	Found in Experiment 1		2,361,076	2,365,214
			2,379,134	2,380,114
			2,394,621	2,397,191
	Found in Experiment 2		2,374,564	2,384,805
			2,394,471	2,395,121
	Shared by Experiment 1 and 2		2,374,564	2,384,805
			2,394,471	2,397,191
	Previously mapped origin	*LMNB2* ori	2,379,085	2,379,352
HBB	Found in Experiment 1		5,209,792	5,210,818
			5,219,144	5,223,314
	Found in Experiment 2		5,184,279	5,187,132
			5,202,479	5,206,232
			5,210,198	5,211,028
			5,217,893	5,221,058
	Shared by Experiment 1 and 2		5,209,792	5,211,028
			5,217,893	5,223,314
	Previously mapped origins	HBB ori 1	5,205,800	5,210,392
		HBB ori 2 (<650-850 bp)	5,225,895	5,226,050
FRAXA	Found in Experiment 1		146,633,555	146,636,361
			146,643,636	146,646,229

			146,696,368	146,700,876
			146,707,372	146,708,160
			146,717,549	146,719,069
			146,728,517	146,731,718
			146,743,855	146,747,268
			146,751,581	146,753,686
			146,780,483	146,781,523
			146,811,457	146,812,372
			146,816,470	146,819,096
	Found in Experiment 2		146,643,636	146,647,759
			146,696,368	146,702,766
			146,706,006	146,706,896
			146,714,362	146,719,459
			146,740,713	146,747,268
			146,780,483	146,782,891
			146,816,470	146,820,884
	Shared by Experiment 1 and 2		146,643,636	146,647,759
			146,696,368	146,702,766
			146,706,006	146,708,160
			146,714,362	146,719,459
			146,740,713	146,747,268
			146,780,483	146,782,891
			146,816,470	146,820,884
	Previously mapped origin	*FMR1* ori	146,698,529	146,699,029
Chr22	Found in Experiment 1		28,968,247	28,969,137
			28,994,037	28,994,976
			29,024,407	29,024,995
			29,039,147	29,040,692
			29,059,018	29,059,818
			29,072,440	29,076,714
			29,142,437	29,143,897
			29,150,302	29,150,986
			29,166,462	29,166,999
			29,203,620	29,204,447
			29,311,351	29,312,264
			29,337,477	29,338,217
			29,426,404	29,427,354
			29,432,393	29,433,043
			29,473,704	29,474,894
			29,486,811	29,487,581
			29,520,964	29,521,944

Supplementary Table 2

		29,525,829	29,528,037
		29,530,187	29,531,047
		29,543,826	29,545,057
		29,547,524	29,551,472
		29,603,147	29,603,767
		29,622,826	29,625,126
		29,645,234	29,645,884
		29,650,788	29,657,772
		29,660,345	29,661,603
		29,666,419	29,672,302
		29,674,829	29,678,687
		29,688,494	29,698,952
		29,708,952	29,711,233
		29,811,125	29,811,805
		29,816,089	29,817,039
		29,912,611	29,913,356
		29,916,302	29,917,072
		29,970,575	29,971,015
		29,978,784	29,979,581
		29,990,586	29,992,034
	Found in Experiment 2	28,957,459	28,959,388
		28,962,630	28,969,047
		28,977,343	28,978,040
		29,039,387	29,040,752
		29,044,824	29,046,432
		29,048,888	29,049,598
		29,053,497	29,055,863
		29,061,887	29,065,916
		29,073,129	29,073,749
		29,104,370	29,107,594
		29,142,437	29,145,612
		29,155,004	29,155,683
		29,211,414	29,212,124
		29,263,324	29,264,544
		29,292,486	29,297,403
		29,384,317	29,385,760
		29,415,895	29,416,875
		29,524,374	29,526,584
		29,543,406	29,545,027
		29,547,524	29,548,384
		29,603,147	29,605,216
		29,623,006	29,627,974

Supplementary Table 2

		29,645,534	29,646,154
		29,655,172	29,658,162
		29,666,419	29,669,523
		29,676,987	29,679,764
		29,685,712	29,699,547
		29,709,372	29,711,353
		29,802,008	29,802,996
		29,807,018	29,808,988
		29,811,155	29,813,830
		29,823,896	29,826,960
		29,839,028	29,840,388
		29,843,726	29,845,474
		29,897,875	29,900,021
		29,916,302	29,917,582
		29,925,441	29,926,806
		29,930,773	29,932,712
		29,967,694	29,971,195
		29,978,904	29,979,761
		29,987,590	29,988,300
		29,995,421	29,999,992
	Shared by Experiment 1 and 2	28,962,630	28,969,137
		29,039,147	29,040,752
		29,072,440	29,076,714
		29,142,437	29,145,612
		29,524,374	29,528,037
		29,543,406	29,545,057
		29,547,524	29,551,472
		29,603,147	29,605,216
		29,622,826	29,627,974
		29,645,234	29,646,154
		29,650,788	29,658,162
		29,666,419	29,672,302
		29,674,829	29,679,764
		29,685,712	29,699,547
		29,708,952	29,711,353
		29,811,125	29,813,830
		29,916,302	29,917,582
		29,967,694	29,971,195
		29,978,784	29,979,761

Supplementary Table 2

Supplementary Table 3. Sequence, Chromosomal Coordinates and Amplification Conditions of the Real-Time PCR Primer Sets

Region	Primer	Sequence	Start (bp)	End (bp)	Annealing Temp (^{0}C)	$MgCl_2$ (mM)
MYC	-6.8p forward	gagttggcaacccttgatgt	128,808,885	128,808,904	58	2
	-6.8p reverse	gttaggatttcccgcctttc	128,809,139	128,809,158		
	-0.9p forward	cagcagtttcagaggcaaag	128,814,762	128,814,781	61	3
	-0.9p reverse	cagcagaaggtgatgggtat	128,815,065	128,815,084		
	orip forward	tacagactggcagagagcag	128,816,612	128,816,631	59/60	2
	orip reverse	atgtatgcacagctatctgg	128,816,805	128,816,824		
	+7p forward	ggttctaagatgcttcctgg	128,823,018	128,823,037	59	2
	+7p reverse	tggttgtgaaggcagcagaa	128,823,287	128,823,306		
LMNB2	-5.9p forward	gctgcgctcaggttaagaag	2,372,931	2,372,950	68	2
	-5.9p reverse	gtgctcacggcagataaggt	2,373,161	2,373,180		
	orip forward	gcgtcacagcacaacctgc	2,379,333	2,379,352	62	3
	orip reverse	gaggcagaacctaaaatcaaa	2,379,153	2,379,173		
	+3.6p forward	gttaacagtcaggcgcatgggcc	2,383,142	2,383,164	66	3
	+3.6p reverse	ccatcagggtcacctctggttcc	2,382,924	2,382,946		
	+5.5p forward	ctcctcgatgctgacgctac	2,384,872	2,384,891	68	3
	+5.5p reverse	taccagtcccaccttccttg	2,385,116	2,385,135		
FRAXA	-7.7p forward	ctgggcatggaagtcaagtt	146,688,379	146,688,398	63	2
	-7.7p reverse	gagtgccagtttccaagctc	146,688,633	146,688,652		
	-1.1p forward	actgtaggggaggagggaga	146,695,034	146,695,053	65	2
	-1.1 reverse	tcttttccatggctcaaacc	146,695,287	146,695,306		
	orip_1 forward	acaacagcttacacttggag	146,697,411	146,697,430	62	2
	orip_1 reverse	ctaatagcactgagttggca	146,697,711	146,697,730		
	orip_2 forward	gcgcgtctgtctttcgaccc	146,698,804	146,698,823	64	2
	orip_2 reverse	ccctccaccggaagtgaaacc	146,699,009	146,699,029		
	orip_3 forward	aggtctcctttggcttctct	146,699,760	146,699,779	63	2
	orip_3 reverse	atggttttagacgctgaagc	146,700,045	146,700,064		
	orip_4 forward	ttggggtcaaccacattttt	146,702,529	146,702,548	58	2
	orip_4 reverse	cgatcccaatcttctcagga	146,702,742	146,702,761		
	+1.5 forward	gagcagtggttcctgttggt	146,704,269	146,704,288	68	4
	+1.5 reverse	ctagcaactgggccaaagag	146,704,450	146,704,469		
	+4.9 forward	aaacctgacaccaccctcag	146,707,695	146,707,714	68	3
	+4.9 reverse	ggcctctctccattccttct	146,707,920	146,707,939		
OSPB2	-2.1 forward	gcaacaagggatgtgaggat	29,600,765	29,600,784	60	3
	-2.1 reverse	tggtccaggctaggaaactg	29,600,991	29,601,010		
	orip_1 forward	cagaatcagcaggagggttt	29,603,144	29,603,163	63	2
	orip_1 reverse	agagggaaagatgaccagag	29,603,420	29,603,439		
	orip_2 forward	gcagccagataggcaagaac	29,603,693	29,603,712	65	2

	orip_2 reverse	tctcaaggctcagagtgcaa	29,603,957	29,603,976		
	orip_3 forward	tagcccagaccttcaacacc	29,604,677	29,604,696	62	2
	orip_3 reverse	ctctgagcccacatcctctc	29,604,920	29,604,939		
	+0.4p forward	tgccacatcacctcctgata	29,605,623	29,605,642	60	2
	+0.4p reverse	aacctctggatttgcccttt	29,605,869	29,605,888		
	+2.9p forward	acccctccaagagcttcatt	29,608,136	29,608,155	56	3
	+2.9p reverse	ggacagctgggctcattaaa	29,608,378	29,608,397		
RNF185	-4.3p forward	tgccatgatttggggttatt	29,911,800	29,911,819	56	3
	-4.3p reverse	gtaggccaggacagtggaaa	29,912,007	29,912,026		
	orip_1 forward	cttctcccttggatgtgaa	29,916,151	29,916,170	58	2
	orip_1 reverse	tggagcctctcctgctacat	29,916,389	29,916,408		
	orip_2 forward	caggatctgggtgactttgt	29,916,460	29,916,479	63	3
	orip_2 reverse	agaagttagaggagcaggtg	29,916,745	29,916,764		
	orip_3 forward	cacctgctcctctaacttct	29,916,745	29,916,764	63	2
	orip_3 reverse	aacagagggtgggttgtcag	29,917,107	29,917,126		
	orip_4 forward	ctgacaacccaccctctgtt	29,917,107	29,917,126	62	2
	orip_4 reverse	cgaggaggggtcttctctct	29,917,474	29,917,493		
	+1.1p forward	tttggcaggttttccatgat	29,918,717	29,918,736	61	3
	+1.1p reverse	cagttgggcaacaagagtga	29,918,968	29,918,987		
	+2.4p forward	ctggccttgttgaccaaagt	29,920,006	29,920,025	60	3
	+2.4p reverse	cttgggaaggtgcaattgtt	29,920,205	29,920,224		

The FRAXA orip_2 primer set corresponds to the FraX-1d primer set used by Gray et al (2007). The numbers associated with the primer sets adjacent to the origins correspond to the distance in kb from the boundary of the closest origin. Two to four sets of primers (orip_1 to_4p) were used to verify each of the three novel origins.